![HAL open science logo]

Ultra light-sensitive and fast neuronal activation with the Ca-permeable Channelrhodopsin CatCh

Sonja Kleinlogel, Katrin Feldbauer, Robert Edward Dempski, Heike Fotis, Phillip G Wood, Christian Bamann, Ernst Bamberg

▶ **To cite this version:**

HAL Id: hal-00622878
https://hal.archives-ouvertes.fr/hal-00622878

Submitted on 13 Sep 2011

Ultra light-sensitive and fast neuronal activation with the Ca^{++} permeable Channelrhodopsin CatCh

Sonja Kleinlogel[1], Katrin Feldbauer[1^], Robert E. Dempski[1,2^], Heike Fotis[1], Phillip G. Wood[1], Christian Bamann[1] and Ernst Bamberg[1,3*]

[1]Max-Planck-Institute of Biophysics, Department of Biophysical Chemistry, Max-von-Laue-Strasse 3, D-60438 Frankfurt am Main, Germany

[2]Present address: Department of Chemistry and Biochemistry, Worcester Polytechnic Institute,100 Institute Rd., Worcester, MA 01609, USA

[3]Chemical and Pharmaceutical Sciences Department, Johann-Wolfgang-Goethe-University

Frankfurt, Max-von-Laue-Strasse 1, 7-9, D-60439 Frankfurt am Main, Germany

[*] corresponding author

[^] KF and RED contributed equally

Word count: 3540 (excluding Abstract, Methods, References and Figure legends)

Abstract

The light-gated cation channel channelrhodopsin-2 (ChR2) has rapidly become a principal tool in neuroscience and its use is currently considered in multiple therapeutic interventions. Although wild-type and known variant ChR2s are able to drive light-activated spike trains, their use in potential clinical applications is limited either by low light-sensitivity or slow channel kinetics. Here we present a new variant, CatCh, mediating accelerated response time and a voltage response that is ~70-fold more light-sensitive than that of wild-type. We show that CatCh's superior properties stem from its enhanced Ca^{++}-permeability. An increase in $[Ca^{++}]_i$ elevates the internal surface potential, facilitating activation of voltage-gated Na^+-channels and indirectly increasing light-sensitivity. Repolarization following light-stimulation is markedly accelerated by Ca^{++}-dependent BK-channel activation. Our results demonstrate a new principle, shifting permeability from monovalent to divalent cations, to increase sensitivity without compromising fast kinetics of neuronal activation. This paves the way for clinical use of light-gated channels.

Introduction

The light-gated, inwardly rectifying cation channel channelrhodopsin-2 (ChR2) has become a preferred tool for the targeted light-activation of neurons both in vitro and vivo[1-4]. Although wild-type (WT) ChR2 can be employed for light-induced depolarization, there is an ongoing search for ChR2 mutants with increased light-sensitivity for potential future clinical applications[5-7]. Higher efficacy would enable depolarization of cell layers distant from the applied light source despite the low optical transmittance of brain tissue. An increase in light-sensitivity would also solve the problem of potential cell damage under continuous illumination due to the high blue light intensities required for full WT ChR2 activation (10^{18}-10^{19} ph s^{-1} cm^{-2} at 480 nm). Variants with higher light-sensitivity are also crucial for research pertaining to the recovery of vision[8,9]. On the protein level, higher light efficacy can only be achieved by increasing the life-time of the open state and/or by elevating the unit conductance of the

channel, as the light-sensitivity *per se* can be improved only marginally due to the nature of the ChR2 chromophore retinal. Previous research has demonstrated that mutations at positions C128 and D156 in helix 3 and 4, respectively, resulted in markedly slowed channel kinetics with open life-times up to 30 minutes and more, yielding a 500-fold or even higher light-sensitivity[5,6]. These C128 and D156 mutants can be switched off at variable open times by red light. Despite the superior light-sensitivity, their slow closing kinetics remains a limiting factor for their applicability. Here we chose a different approach: since it is known that a cell's inner membrane surface potential is strongly influenced by Ca^{++}, modifying submembraneous intracellular Ca^{++} levels will lead to depolarization of the membrane and in neurons to activation of voltage-gated Na^+ channels. Thus we hypothesized that the light-sensitivity of a neuron can be indirectly increased by elevating its inner membrane surface potential *via* Ca^{++}-influx[10,11]. We created a ChR2 mutant with an enhanced Ca^{++}-permeability, which we named CatCh, i.e. **Ca**lcium **t**ranslocating **Ch**annelrhodopsin. CatCh has a up to six-fold higher Ca^{++}-permeability, a 70-fold higher light-sensitivity and faster response kinetics when expressed in hippocampal neurons compared to the WT ChR2. The enhanced light-sensitivity and fast kinetics are shown to stem from the relatively high light-gated Ca^{++}-influx, which elevates the inner membrane surface potential and activates Ca^{++}-activated large conductance potassium (BK) channels. CatCh exemplifies a new principle by which light-gated channels can be engineered to increase the light-sensitivity of neuronal stimulation. Its characteristics such as triggering precise and fast action potentials while requiring low light intensities for activation open the way for the use of light-gated channels in clinical applications.

Results

Our objective was to identify residues within WT ChR2 whose mutations modify cation permeability. We focused on the third transmembrane domain as several mutated residues within this domain alter the photocycle and the gating of the channel (**Fig. 1**)[5-7,12]. Each residue from Arg^{115} to Thr^{139} was individually replaced by cysteine and

screened for functional changes in *Xenopus laevis* oocytes. The L132C (CatCh) mutation displayed significant alterations in the amplitude and shape of the current traces.

Molecular properties and selectivity of CatCh

In HEK293 cells, the blue light-induced stationary currents of CatCh had a ~2.5-fold higher amplitude compared to WT ChR2 (CatCh: 25.0 ± 8.8 pA/pF; WT: 10.1 ± 4.1 pA/pF; mean ± s.d., n=6, -60 mV). The steady-state to peak-current ratio also increased from 0.37 ± 0.18 in the WT to 0.60 ± 0.20 in CatCh (**Fig. 2a**). During repetitive blue-light stimulation the CatCh peak current disappeared. It recovered within minutes in the dark, when recovery was not prematurely induced by yellow light. In contrast, a full recovery of the WT ChR2 peak current under identical conditions takes 20 seconds[13]. Activation and deactivation time constants of CatCh (τ_{on} = 590 ± 3 μs, τ_{off} = 16 ± 3 ms, n=9, pH 7.4, -60 mV, mean ± s.d.) were slightly longer compared to WT ChR2 (τ_{on} = 214 ± 2 μs, τ_{off} = 10 ± 1 ms, n= 9, pH 7.4, -60 mV; mean ± s.d.; **Fig. 2b**, **Supplementary Fig. 1** bottom panel, **Table 1**).

Next we compared the described effects on the channel properties to the spectral changes in the photocycle. Flash photolysis experiments on purified CatCh revealed only minor deviations from the WT ChR2 spectra[13] (**Supplementary Fig. 1**). 1. The early P390 intermediate, which represents the deprotonated Schiff base, is barely detectable. 2. The intermediate P520, which represents the open state of the channel, shows a slightly lengthened life-time of 9 ms, comparable to the τ_{off} value determined electrophysiologically. Similar open life-time values were obtained for the mutant H134R, which showed doubled activity at unchanged unit conductance[2,14]. Therefore, also in the case of CatCh, the decelerated kinetics of the open state could be responsible for the 2.5-fold increased stationary currents measured in HEK293 cells, whereby the unit conductance remains unchanged. This was confirmed by measuring the single channel conductance of CatCh as previously described[14]. In line with the WT ChR2 and H134R noise analysis experiments, guanidine was used as conducting ion. Note that the kinetic properties of the channel are independent on the permeating cation[14]. The evaluation of difference power spectra yielded a single channel conductance γ of 140 ± 5 fS (n=6,–60

mV) for 200 mM guanidine at room temperature (23°C), which is similar to the extrapolated room temperature WT ChR2 single channel conductance of 150 fS[14]. The open probability of CatCh determined from the noise analysis is unchanged in comparison to H134R ($P_o \sim 0.6$). Thus, an increased open channel life-time can easily account for the observed increase in photocurrents by a factor of 2.5, however, a slightly enhanced expression of CatCh copies cannot be excluded.

Excitation of CatCh with varying wavelengths in *Xenopus laevis* oocytes revealed an almost identical action spectrum to the WT ChR2 spectrum with a maximum excitation wavelength at 474 nm (**Supplementary Fig. 2**). In the presence of extracellular Ca^{++} and at negative holding potentials, CatCh currents showed a dramatic increase in amplitude during illumination due to a superimposed outward current which resembles that of calcium activated chloride channels (CaCC)[15,16] (**Fig. 2c**). In WT ChR2-expressing oocytes CaCC currents were also observed, but they were markedly smaller than those induced by CatCh (**Fig. 2c**). For both, WT ChR2 and CatCh, at 80 mM extracellular Ca^{++}, injection of the fast Ca^{++} chelator BAPTA 1,2-bis(2-aminophenoxy)ethane-N,N,N',N'-tetraacetate into the cell abolished the CaCC currents, while a residual Ca^{++} current remained (**Fig. 2c**)[1]. The larger difference of the photocurrents before and after BAPTA injection for CatCh supports the hypothesis of an increased Ca^{++}-flux following CatCh activation.

Increased calcium permeability of CatCh

In order to obtain an estimate of the CatCh ion permeability, photocurrent-voltage relationships and the reversal potential for different cations were measured in HEK293 cells. These experiments revealed that the permeabilities for sodium, potassium and magnesium are comparable to WT ChR2 (**Fig. 2d**)[1]. The proton permeability of CatCh ($p_H/p_{Na} = 4\times10^6$) is slightly increased compared to WT ChR2 ($p_H/p_{Na} = 2.5\times10^6$). The relative Ca^{++} permeability of CatCh p_{Ca}/p_{Na} is increased from 0.15 in WT to 0.24 as evidenced from the shift in the reversal potential as going from sodium to calcium in the extracellular solution (bi-ionic potential). The shift is smaller for Catch (–21.6 mV, mean ± s.d., n=5) compared to the WT (–30.7 mV, mean ± s.d., n=5) as shown in figure 2e.

In order to further quantify the increased Ca^{++}-permeability of CatCh, we performed Fura-2 calcium imaging on CatCh-expressing HEK293 cells and compared the measured 340/380 ratios to the ratios measured in WT ChR2-expressing cells. To exclude varying CatCh expression levels as a factor in calcium uptake, the measured 340/380 ratios were normalized to the YFP-fluorescence value of each individual cell (see methods for details). Figure 2f shows that upon a 10-s blue-light (460 nm) photostimulation in saturating 90 mM Ca^{++} solution the increase in intracellular free Ca^{++} in CatCh-expressing cells is about 6-times larger than in WT-expressing cells but remains, however, in the nanomolar range.

Application to hippocampal neurons

To test CatCh's suitability for neuronal application, we transduced the construct with the help of adeno-associated viruses into cultured hippocampal pyramidal cells. The CatCh mutant was robustly expressed (**Fig. 3a**) without signs of neurotoxicity for the life-time of the culture (~5 weeks) and exhibited in whole-cell recordings, as in HEK293 cells, a higher steady state-to-peak ratio and about 3.5-fold increased current amplitudes compared to the WT (CatCh: 8.0 ± 0.4 pA/pF; WT 2.3 ± 0.5 pA/pF; -60 mV, n=6, mean ± s.d.; **Fig. 3b**). In current clamp mode, artificially high light intensities typically used to activate the WT (10^{18}–10^{19} photons s^{-1} cm^{-2}) drove CatCh-expressing pyramidal cells into a depolarization block (**Fig. 4a**). To induce reliable spike trains, the light intensity was reduced by 2 log units (5 x 10^{16}–2 x 10^{17} photons s^{-1} cm^{-2}) to a light intensity within the natural range of cone photoreceptor driven photopic vision (**Fig. 4b**)[17]. Figure 4c shows a representative tuning curve for the light-intensity dependent firing rate of a pyramidal cell. The averaged maximum firing rate lies at 8.2 x 10^{16} ± 2.5 x 10^{16} photons s^{-1} cm^{-2} (mean ± s.d., n=5). The higher light efficacy of CatCh-expressing neurons facilitates activation with wavelengths away from the peak sensitivity, as exemplified for green light (532 nm) in figure 4d. This may confer benefits in terms of more effective tissue recruitment with deeper-penetrating green light. We assign the dramatically enhanced light-sensitivity of CatCh-expressing neurons to an increased Ca^{++} permeability, thereby transiently increasing the surface potential on the cytosolic membrane surface[10,11,18,19] (for an explanation of the Ca^{++} effect on the surface potential see **Supplementary Figure**

3). During light excitation, CatCh serves as a membrane bound fast Ca^{++}-source that temporarily increases the local intracellular surface-Ca^{++}-concentration and neutralizes the negative membrane surface charges. It is known that this causes a shift of the internal surface potential to more positive values, thus depolarizing the membrane[11,18]. A consequence is that voltage-gated Na^+-channels are activated at more negative membrane potentials[18]. After short light pulses or after switching off the stationary light, Ca^{++} equilibrates rapidly (microseconds) within the cytoplasm, leading to a rapid recovery and the immediate disappearance of action potentials. Thus, for CatCh, less photocurrent and subsequently less light is required for spike initiation compared to WT ChR2. The light pulse-to-spike latency in CatCh was faster (~ 5-6 ms; **Fig. 4e**) with a smaller jitter than the latency for WT ChR2 (~10 ms) at identical light intensities (2.8×10^{18} photons s^{-1} cm^{-2})[3]. We further tested CatCh for its ability to induce single action potentials at high frequency light-stimulation. A train of 1-ms 473-nm light pulses (2.8×10^{19} photons s^{-1} cm^{-2}) drove 100% reliable spike trains up to frequencies of 50 Hz (n=8; **Fig. 4f** - most pyramidal cells do not follow well beyond 50 Hz even with direct current injection). The WT, on the other hand, requires at least 2-ms light pulses to induce spikes and does this reliably only up to frequencies of 20 Hz[12]. We pushed the short activation times of CatCh even further and evoked single action potentials up to frequencies of 10 Hz by 10 ns blue light pulses (1.1×10^{25} photons s^{-1} cm^{-2}), a pulse length so short to only induce a single turnover in each CatCh protein (**Fig. 4g**). However, fast stimulation frequencies also require a fast repolarization of the cell after each spike. Despite a decelerated τ_{off} of CatCh compared to the WT, the ~6-fold increased Ca^{++}-influx during CatCh activation (see Fura-2 measurements **Fig. 2f**) appears to suffice to activate enough Ca^{++}-activated large conductance potassium channels (BK channels)[20] to potently repolarise the cell to its original resting potential within milliseconds after each action potential. To prove that the fast repolarization was mediated through BK channels, we added 100 μM of the potassium channel inhibitor tetraethylammonium (TEA) to the extracellular solution and observed incomplete membrane repolarization and the generation of a plateau potential typically seen in pulse stimulation protocols with the WT ChR2[3] (**Fig 4h**).

Taken together, CatCh-expressing neurons exhibit a faster spike onset, a faster repolarization and an increased light-sensitivity compared to WT-expressing cells (for a

comparison see table 1). Control experiments in the absence of external Ca^{++} and in the presence of 3 mM Mg^{++}, which has a less pronounced effect on the surface potential[11,18] (**Supplementary Fig. 3**) and is not conducted through WT ChR2 or CatCh, support the above interpretations: 1. The light pulse-to-spike latency increased to WT ChR2 values (**Fig. 4e**), 2. Instead of the fast spike repolarization as observed in the presence of Ca^{++}, a prolonged artificial depolarization similar to what is seen in WT ChR2 experiments was observed (**Fig. 4i**, left), 3. In the absence of Ca^{++}, identical light intensities resulted in a reduced depolarization by ~ 10 mV under otherwise equal experimental conditions and 4. Multi-spiking as expected from the prolonged open time of CatCh reoccurs in the absence of Ca^{++} (**Fig. 4i**, right).

We performed further control experiments to rule out potential detrimental consequences of the higher Ca^{++} permeability of CatCh on cell health, especially following prolonged stimulation: 1. Repetitive stationary or high-frequency illumination did not induce changes in CatCh responses nor in membrane resistance, membrane capacitance or leak currents, 2. Exposure to hourly 50 Hz blue-light pulse-trains for 10 hours did not affect neuronal health.

To summarize, we have demonstrated that the elevated Ca^{++}-permeability of CatCh pairs increased light-sensitivity with precise spiking control in a higher frequency bandwidth and thus outperforms the WT ChR2 and the published slow and fast mutants (for a comparison of the properties of different ChR2 variants see table 1).

Discussion

At first glance CatCh, the L132C mutant of WT ChR2, shows rather unspectacular results in comparison to the WT ChR2: 1. a two-fold increase of the life-time of the open state, 2. a decelerated decay of the P520 intermediate in the photocycle kinetics, 3. an unchanged single channel conductance and 4. a marginally red-shifted absorption maximum (4 nm). A 2.5-fold increased photocurrent can be easily explained by the measured parameters with no relevant increase in expression level. At second glance, however, closer inspection of the voltage-clamp data obtained from CatCh expressing *Xenopus laevis* oocytes gave a first indication towards an elevated Ca^{++}-permeability, which was then confirmed by the determination of the reversal potential

and calcium imaging experiments on HEK293 cells. Looking at the model in figure 1, an increase in Ca^{++}-permeability might be facilitated by the formation of a more flexible structure and thus the formation of a cavity, as shown for the L94A mutation of the light-driven proton pump bacteriorhodopsin (compare **Fig. 1**)[21]. This cavity would be located in a hydrophobic patch as part of the conserved transmembrane helix three (TM3), only a helical turn apart from C128. Manipulating the interaction between C128 (TM3) and D156 (TM4) decelerates the reaction cycle of ChR2 dramatically[5,6], an effect that was also observed in the bacteriorhodopsin mutant L93A[22,23], i.e. the neighboring residue of L94. In ChR2, the interaction of TM3 and TM4 seems to affect both gating and selectivity, pointing to a structural element as transducer of the light reaction to the ion pore[24]. Insertion of the smaller and more hydrophilic cysteine could increase the flexibility of the helical segment, facilitating the access of Ca^{++}.

When delivered to hippocampal pyramidal cells, CatCh exhibited a ~70-fold increase in light-sensitivity compared to WT ChR2. Usually, such an increased light efficacy is accompanied by a strongly prolonged open channel life-time[2,6,13]. This is not the case for CatCh. Instead, the secondary effects on neuronal excitability are induced by Ca^{++}-influx through CatCh. Before we discuss the mechanism, we elucidate possible drawbacks of the elevated Ca^{++}-flux.

At resting membrane potential, Ca^{++} has a low contribution to the overall current in neurons that is mainly driven by sodium and protons. The Ca^{++} contribution estimated from the Goldman-Hodgkin-Katz-equation is less than one percent (Supplementary Note). In the neuron experiments, the total current density is given by 8.0 pA pF^{-1}; hence the calcium current density is 0.06 pA pF^{-1} (Supplementary Note). Simplified geometric considerations of the neuron, i.e. spherical soma and cylindrical dendrites, give an estimate of the rate of $[Ca^{++}]$ change of 1 and 12 µM s^{-1} in the soma and the dendrites, respectively (Supplementary Note). This is lower than the fluxes e.g. through NMDA receptors[25] and detrimental effects on cell health by the calcium flux *per se* seem unlikely. This notion is further corroborated by our control experiments. The raise in intracellular Ca^{++} levels during repetitive CatCh stimulation is too small to affect cell health. Nonetheless, the study of long-term effects of CatCh activity on neuronal health,

plasticity (Supplementary Discussion) and signaling cascades using CatCh-expressing transgenic animals are essential for the future.

How can we account for the increased light-sensitivity in neurons? The best interpretation of the mechanism underlying the observations is based on the increased Ca^{++}-influx into the neuron during illumination. This temporarily neutralizes the negative charges on the inner membrane face, thereby increasing the surface potential, which is equivalent to a depolarization of the membrane[11] (**Supplementary Fig. 3**). This screening effect is well known for the extracellular leaflet of the membrane that affects activation of the voltage-gated sodium channels[10,18]. Here, we can consider CatCh as a light-gated membrane bound Ca^{++} source ("a membrane bound caged Ca^{++}"), which transiently delivers Ca^{++} to the cytosolic surface of the cell membrane as long as the CatCh channel is open. This facilitates the activation of voltage-gated sodium channels, which appears as an increase in light-sensitivity. However, it is the transient Ca^{++} binding to the inner membrane surface that increases light-sensitivity and not the marginally elevated Ca^{++} concentration in the cytosol. When extracellular Ca^{++} was replaced by the non-permeating Mg^{++}, all the observed Ca^{++} effects on the action potential were abolished. This proves that the observed Ca^{++} effects were due to influx of extracellular Ca^{++} and not caused by a rise of the intracellular $[Ca^{++}]$ through a potential expression of CatCh in the cell organelles like the endoplasmatic reticulum.

Despite having a longer lifetime of the open state compared to the WT ChR2, CatCh shows increased spike-reliability and precision during high-frequency light-stimulation, reducing extra spikes and eliminating artificial plateau potentials typically observed in WT-expressing cells at stimulation frequencies above 20 Hz[3,7,12]. 10-ns to 1-ms light pulses delivered at room temperature induced reliable spike trains up to 50 Hz in CatCh-expressing pyramidal cells (their limit of natural spiking; **Fig. 4f**). As demonstrated in the result section, the fast spiking might be caused by the calcium induced BK channels which repolarize the cells. This re-establishes the resting membrane potential of the neuron within milliseconds after each action potential and represents the second calcium mediated effect that is controlled by CatCh activity. Higher frequency spiking may be achieved in faster spiking cells such as cortical paravalbumin interneurons[12].

In comparison to already available optogenetic tools, CatCh induces in neurons an increased light-sensitivity similar to the slow-mutants[13] or SFO's[6] but with much accelerated response kinetics owing to its increased Ca^{++}-permeability and the consequences on neuronal excitability. This makes CatCh superior to available ChR2 variants, where a high light-sensitivity had to be established at cost of fast kinetics and *vice versa* with respect to the fast channelrhodopsins[7,12] (see table 1).

With regard to optogenetic application, we note that it will be important to validate the optimal light-pulse parameters in each experimental preparation such as stimulation length and intensity, as the specific response will ultimately be controlled by intrinsic properties of the neuron and CatCh expression levels.

The possibility to activate CatCh with naturally occurring light intensities whilst maintaining high temporal precision makes it an important candidate particularly for gene-therapeutic visual restoration efforts[26] but also other biomedical applications. Due to its reduced light-requirements, CatCh spikes can be generated even by excitation far from its spectral maximum of 474 nm, e.g. with green light (**Fig. 4d**), facilitating tissue penetration.

There are additional potential fields of application for CatCh, since, as demonstrated for BK-channels, other Ca^{++}-sensitive processes may be transiently triggered at the membrane during illumination (Supplementary Discussion). Further, the combination of CatCh with the so far characterized ChR2 variants, e.g. ChETA or the slow mutants, might further improve optogenetic tools.

Acknowledgements

Author contributions

S.K., R.E.D., P.G.W. and E.B. conceived the experiments, S.K., K.F., H.F. and C.B. carried them out; S.K., C.B. and K.F. carried out the data analysis; S.K., C.B. and E.B. wrote the paper.

Figure Legends

Figure 1 Homology model of ChR2 based on the Sensory Rhodopsin 2 structure (PDB code 1H2S). The target region for the cysteine scanning (R115 to T139) is located in the transmembrane helix 3 (TM3) and is highlighted in red. The inset shows the presumable location of the mutated L132C, the hydrogen-bonded C128 and D156, connecting TM3 and TM4 as indicated by the dotted line, and the homologue residues for the proton donor (H134) and proton acceptor (E123), respectively. The chromophore is formed by all-*trans* retinal (ATR) and K257 covalently linked by a Schiff-base. The cavity formed by the removal of the leucins's methyl groups is depicted as spheres and overlaid on the mutated sulfhydryl group of the cysteine residue (yellow ball).The figure was prepared with VMD[27].

Figure 2 Biophysical characterization of CatCh in HEK293 cells and *Xenopus* oocytes. **(a)** Photocurrents in response to a 1-s blue light pulse. Traces are normalized to the peak photocurrent amplitude to illustrate the increase in the steady state-to-peak current ratio in CatCh compared to the WT. **(b)** Comparison of on-kinetics (left) and off-kinetics (right) of photocurrents normalized to peak and steady-state currents, respectively. **(c)** Typical responses to a 600-ms blue light pulse of CatCh and WT ChR2 expressing *Xenopus* oocytes in 80 mM extracellular Ca^{++} (pH 9) at -120 mV (continuous lower traces). Injection of 1 mM BAPTA (Ca^{++} chelator) abolished the superimposed currents of the intrinsic Ca^{++}-activated chloride channels, while residual channelrhodopsin Ca^{++}-currents remained (dashed upper traces). Currents were normalized to the WT ChR2 peak current. **(d)** Ion flux characteristics of CatCh in HEK293 cells at -80 mV (mean $\pm$ s.d., n=6). **(e)** Shift of the reversal potential (E_r) for WT ChR2 (-●-) and CatCh (-■-) when exchanging the extracellular solution from 140 mM Na^+ (-▲-, WT and CatCh are superimposed) to 90 mM Ca^{++}. The intracellular solution is kept constant with 140 mM Na^+ inside that leads to a negative E_r in the presence of Ca^{++} (mean $\pm$ s.d., n=5). **(f)** Fura-2 measurements of Ca^{++}-influx in HEK293 cells expressing WT ChR2 (●) and CatCh (■) to 10 s of 460-nm light in the presence of 90 mM extracellular Ca^{++} (n=10). The

fluorescence ratios at 340/380 are normalized to the YFP fluorescence (see methods). Control untransfected HEK293 cells (▲).

Figure 3. CatCh-expression in hippocampal cultured neurons. **(a)** Confocal image of a cultured hippocampal neuron expressing ChR2(L132C)-2A-EGFP under the CAG promoter. Scale bar 20 μm. **(b)** Typical photocurrents at -60 mV of CatCh and WT ChR2 evoked by blue light (J_{473nm} 1×10^{19} photons s^{-1} cm^{-2}).

Figure 4 Fast and high-sensitivity neural photostimulation. **(a-d)** Representative whole cell current-clamp recordings from a CatCh-expressing hippocampal neuron in response to 2-s light pulses. **(a)** The blue light intensity required for the WT induces a depolarization block (J_{473nm} 2.5×10^{17} photons s^{-1} cm^{-2}). **(b)** Reducing the light intensity by a factor 10 re-establishes firing (J_{473nm} 2.5×10^{16} photons s^{-1} cm^{-2}). **(c)** Representative light-tuning curve for spike-firing (J_{max} 9.7×10^{16} photons s^{-1} cm^{-2}, mean ± s.d.). **(d)** Moderate green illumination also evokes trains of action potentials (J_{532nm} 2.5×10^{17} photons s^{-1} cm^{-2}). **(e)** Light pulse-to-spike peak latency throughout light pulse trains consisting of 25 1-ms 473-nm light pulses (J_{473nm} 3×10^{18} photons s^{-1} cm^{-2}, mean ± s.d. [jitter]), in 2 mM extracellular Ca^{++} (□) and as control at 5 Hz in 3 mM extracellular Mg^{++} (●), which increases latency to values similar of WT ChR2. **(f)** Spike firing in response to 1-ms 473-nm pulses (grey bars) at a rate of 50 Hz (J_{473nm} 2.8×10^{19} photons s^{-1} cm^{-2}) and **(g)** in response to 10 ns 473-nm light pulses at 10 Hz (J_{473nm} 1.1×10^{25} photons s^{-1} cm^{-2}). **(h)** Incomplete membrane repolarization (double-headed arrow) due to inhibition of BK channels by 1 mM TEA applied during a 1-ms 473-nm light pulse train. Overlay of spike before (black) and 1st (red) and 3rd (blue) spikes, respectively, after TEA application (J_{473nm} 1.8×10^{18} photons s^{-1} cm^{-2}). **(i)** Replacement of 2 mM Ca^{++} by 3 mM Mg^{++} in the extracellular solution causes prolonged depolarization (5 Hz, left) and the formation of multiple spikes at higher 473-nm light pulse frequencies (20 Hz, right; J_{473nm} 8.3×10^{18} photons s^{-1} cm^{-2}).

Methods

Spectroscopy. CatCh was expressed in *Pichia pastoris* as described before[5,13]. Flash-photolysis studies were performed in a home-built setup and absorbance changes were measured after excitation of a 10 ns laser flash from an excimer pumped dye laser (450 nm, 2-3 mJ)[13].

HEK293 cell culture and molecular biology. The L132C point mutation of the C-terminally at amino acid 309 truncated cop4 gene (ChR2) fused to YFP (ChR2(L132C)-YFP; vector: *pcDNA3.1(-)-ChR2(L132C)-EYFP*) was transfected in HEK293 cells and kept under G418 selection (0.6 mg/ml; PAA Germany, Cölbe, Germany) at all times to obtain a semi-stable HEK293-CatCh-YFP cell line. For the WT ChR2, the C-terminally truncated ChR2-YFP (vector: *pcDNA4TO-ChR2--EYFP*) was stably transfected into HEK293-Trex cells (Invitrogen) to obtain a tetracycline-inducible stable HEK293-WTChR2-YFP cell line as described[13]. The peak to stationary relations were determined from HEK293 cells transiently transfected (Effectene, QIAGEN) with human-codon-optimized *pcDNA3.1(-)-chop2-EYFP* constructs (WT, H134R or L132C) 24 hours prior to measurements.

Electrophysiological recordings on HEK293 cells. Patch pipettes with resistances of 2-4 $M\Omega$ were fabricated from thin-walled borosilicate glass (GB150-8P, Science Products, Hofheim, Germany) on a horizontal DMZ-Universal puller (Serial No. 5318904120B, Zeitz-Instruments, Augsburg, Germany). Photocurrents were recorded with the whole-cell patch-clamp method and activated by light pulses from a diode-pumped solid-state laser (Pusch Opto Tech GmbH, Baden Baden, Germany; $\lambda = 473$ nm) focused into a 400 μm optic fiber. Light pulses were applied by a fast computer-controlled shutter (Uniblitz LS6ZM2, Vincent Associates). All light intensities given are measured at the end of the light-guide. To get an estimate of the permeability for different cations, we measured photocurrent-voltage relationships and determined the reversal potential. The intracellular solution contained 140 mM NaCl, 7 mM EGTA, 2 mM $MgCl_2$ and 10 mM Tris (pH=9) and the extracellular solution contained 140 mM NaCl, 2 mM $MgCl_2$ and 10 mM Tris (pH=9). For cation permeabilities, external 140 mM NaCl was exchanged by 140 mM KCl, 90 mM $CaCl_2$ or 90 mM $MgCl_2$, respectively. Proton permeabilities were

determined from the reversal potential shift of the current-voltage-relationship when the pH was reduced from 9 to 7.4 (or 6). Permeability ratios were calculated according to the Goldman-Hodgkin-Katz (GHK) equation, including terms for Na^+, K^+, H^+ and Ca^{++}.

Noise Analysis. Experiments were performed on HEK293 cells as described previously[14] and conducted at room temperature (23°C). The pipette solution contained 1 mM Guanidine-HCl, 199 mM NMG-Cl (N-Methylglucamine), 10 mM EGTA, 2 mM $MgCl_2$, and 20 mM Hepes (pH 7.4), the bath solution contained 200 mM guanidine-HCl, 2 mM $MgCl_2$, 2 mM $CaCl_2$, and 20 mM Hepes (pH 7.4). Current response to a blue light stimulus was recorded under application of a voltage step protocol under saturating light conditions and again under light conditions where the current response at –60 mV was half the maximal current ($I_{0.5}$; 2 kHz low-pass Bessel filter; sampling rate: 100 kHz; cell diameter: 15 µm). Recordings of the stationary $I_{0.5}$ during prolonged illumination (2 min) at –60 mV holding potential were used to estimate the conductance of the single channel (2 kHz low-pass Bessel filter; sampling rate 20 kHz). Alternating recordings without (control, 3 recordings) and with illumination (2 recordings, 30 sec after the onset of the light stimulus) were collected, Fourier transformed and the single channel conductance estimated from an approximation with a Lorentzian function[14]. The lower light intensities were chosen in order to obtain the maximal fluctuation of the opening and closing of the light-gated channel.

Fura-2-imaging on HEK293 cells. Fura-2 AM (5 mM; Invitrogen) was loaded at room temperature for 30 min to 1 hour. After loading the cells were recovered in a 140 mM NaCl solution without Ca^{++} (140 mM NaCl, 7 mM EGTA, 2 mM $MgCl_2$ and 10 mM HEPES). Yellow fluorescent protein was excited by a 500 ms exposure to light using a 460/40 nm filter (Visitron Systems, Puchheim, Germany) to estimate each cell's expression level from its YFP-fluorescence. Protein expression levels of the stable HEK293-WTChR2-YFP cell line were ~1.5 increased compared to the semi-stable HEK293-CatCh-YFP cell line. The solution was then replaced by an extracellular Ca^{++}-solution that consisted of 90 mM $CaCl_2$, 7 mM EGTA, 2 mM $MgCl_2$ and 10 mM HEPES. After 15 min in the dark the light-gated channels were stimulated for 10 s with blue light (460/40 nm). Fura-2 was excited with 340 nm (340/20) and 380 nm (380/20) and the emitted light (540/80 nm) detected with a CCD camera (all filters from Visitron Systems,

Puchheim, Germany). A calibration for the intracellular free Ca^{++} was performed with a Fura-2 calcium imaging calibration kit (Invitrogen).

Fura-2 340/380 ratios were determined using MetaFluor software from background corrected fluorescence intensities at 340 and 380 nm excitation. To estimate intracellular free Ca^{++}, the averaged 340/380 fluorescence ratios were compared to a titration curve. Subsequently, the light-induced calcium changes were corrected for the lower expression level in the CatCh expressing cells by normalizing to the YFP fluorescence of the WT expressing cells. Typically, expression of the WT was higher by a factor of ~1.5 and the plotted fluorescence ratios were scaled for the CatCh mutant according to the calibration curve.

***Xenopus laevis* oocyte preparation and molecular biology.** A C-terminally-truncated ChR2 variant (residues 1-315) without extracellularly exposed cysteine residues (containing mutations C34A and C36A) were subcloned into the vector pTLN[28]. Single cysteine mutations were introduced by QuickChange Site-Directed Mutagenesis (Stratagene) and verified by sequencing. The mRNA was prepared using the SP6 mMessage mMachine kit (Ambion, Austin, TX). 50 nl cRNA, which included 30 ng of WT ChR2/CatCh mRNA were injected into each *Xenopus* oocyte. Oocytes were obtained by collagenase treatment after partial ovarectomy. After cRNA injection, oocytes were incubated in all-trans retinal (1 µM, from a 1 mM stock in ethanol) and were kept in ORI buffer (90 mM NaCl, 2 mM KCl, 2 mM $CaCl_2$ and 5 mM Mops, pH 7.4) containing 1 mg/ml gentamycin at 18° C for two to four days.

Two-electrode-voltage clamp on *Xenopus laevis* oocytes. Photocurrents were activated with a 75-W xenon arc lamp and a 450 ± 25 nm band filter, the light of which was coupled into a 1-mm-light-guide with an output of ~10^{18} photons s^{-1} cm^{-2}. Action spectra were recorded using narrow bandwidth filters (398-645 nm; ± 10 nm; K-series Balzer) in combination with neutral density filters to achieve a fiber output of ~ 1.4×10^{17} photons s^{-1} cm^{-2} for each wavelength. For action spectra generation, Ca^{++} in the ORI solution was replaced by Ba^{++} to suppress calcium-activated chloride channel (CaCC) currents. Current amplitudes at each wavelength were normalized to represent equal photon exposure. The ground spectrum determined by spectroscopy was then fitted to the

averaged data points. To suppress CaCC activation, 50 nl of a 20 mM solution of the fast Ca^{2+}-chelator 1,2-bis(2-aminophenoxy)ethane-N,N,N',N'-tetraacetate (BAPTA) was injected into each oocyte (~ 1 mM final concentration in the oocyte).

Hippocampal neuron culture. Hippocampi were isolated from postnatal P1 Sprague-Dawley rats (Jackson Laboratory) and treated with papain (20 U ml^{-1}) for 20 min at 37˚C. The hippocampi were washed with DMEM (Invitrogen/Gibco, high glucose) supplemented with 10% fetal bovine serum and triturated in a small volume of this solution. ~ 75,000 cells were plated on poly-D-lysine / laminin coated glass cover slips in 24-well plates. After 3 hours the plating medium was replaced by culture medium (Neurobasal A containing 2% B-27 supplement, 2 mM Glutamax-I and 100 U/ml penicillin and 100 μg/ml streptomycin). ChR2(L132C)-YFP and ChR2-YFP were transfected 5-10 days after plating using the lipofectamine 2000 reagent (Invitrogen). Alternatively, 2-5 × 10^9 GC/ml of virus (*rAAV2/7-CAG-ChR2(L132C)-2A-EGFP-WPRE-bGH*) was added to each well 4-9 days after plating. Expression became visible 5 days post-transduction. No neurotoxicity was observed for the lifetime of the culture (~5 weeks). No all-trans retinal was added to the culture medium or recording medium for any of the experiments described here.

Adeno-associated viral vector construction. The cytomegalovirus early enhancer / chicken β-actin (CAG) promoter was PCR-amplified and inserted into *pAAV2-Rho-EGFP* (kind gift from Alberto Auricchio[29]) to obtain *pAAV2-CAG-EGFP*. The *pAAV2-CAG-EGFP* viral expression plasmid contained additionally a woodchuck posttranscriptional regulatory element (WPRE) and a bovine growth hormone (BGH) polyadenylation sequence. ChR2(L132C)-2A-EGFP (kind gift from Volker Busskamp – 2A self-cleaving peptide / CHYSEL[30]) was constructed by adapter PCR and subcloned into *pAAV2-CAG-EGFP* by replacement of EGFP using Clontech's in fusion kit. The viral vector (*pAAV2-CAG-ChR2(L132C)-2A-EGFP-WPRE-bGH*) was packaged (serotype 7) and affinity purified at the Gene Therapy Program of the University of Pennsylvania with a final infectious virus titer of 2.26x10^{11} genome copies / ml.

Electrophysiological recordings from hippocampal neurons. For whole-cell recordings in cultured hippocampal neurons, patch pipettes with resistances of 5-10 MΩ

were filled with 129 mM potassium gluconate, 10 mM HEPES, 10 mM KCl, 4 mM MgATP and 0.3 mM Na_3GTP, titrated to pH 7.2. Tyrode's solution was employed as the extracellular solution (125 mM NaCl, 2 mM KCl, 2 mM $CaCl_2$, 1 mM $MgCl_2$, 30 mM glucose and 25 mM HEPES, titrated to pH 7.4). The nominally Ca^{++}-free extracellular solution contained this same solution except that it had 0 mM Ca^{++} and 3 mM Mg^{++}. Recordings were conducted in the presence of the excitatory synaptic transmission blockers, 1,2,3,4-tetrahydro-6-nitro-2,3-dioxo-benzo[f]quinoxaline-7-sulfonamide (NBQX, 10 μM, Sigma) and D(−)-2-Amino-5-phosphonopentanoic acid (AP-5, 50 μM, Sigma). For voltage-clamp recordings 1 μM tetrodotoxin was added to the extracellular solution. To inhibit BK-channel activity, 1 mM TEA was added. Recordings were conducted on an inverted Zeiss Axiovert 25 microscope equipped with a fluorescence lamp. Successful protein expression was proved by EGFP- or YFP-mediated fluorescence. Neuronal access resistance was 15-40 MΩ and was monitored for stability throughout the experiment. Electrophysiological signals were amplified using an Axopatch 200A amplifier (Axon Instruments, Union City, CA), filtered at 10 kHz, digitized with an Axon Digidata 1600 (50 Hz) and acquired and analyzed using pClamp9 software (Axon Instruments). Photocurrents were evoked using light pulses of various lengths from diode-pumped solid-state lasers (Pusch Opto Tech GmbH; λ_1 = 473 nm, P_1 = 100 mW, λ_2 = 532 nm, P_2 = 50 mW) or 10 ns flashes from an excimer pumped dye laser (Coumarin 2, λ = 450 nm). Specific light intensities are indicated in the figure legends and the text and are intensities at the end of a 400 μm diameter quartz optic fiber (STE-F100/400-Y-VIS/NIR; Laser 2000, Wessling, Germany) at a distance of ~500 μm from the cell. Currents measured from neurons expressing ChR2(L132C)-YFP and ChR2(L132C)-2A-EGFP were identical.

Confocal imaging. For imaging, cover-slips with hippocampal neurons were fixed at 4°C for 10 min in 4% paraformaldehyde in PBS buffer containing 2% sucrose. The cells were subsequently incubated for 1.5 hours in rabbit α-GFP IgG (Invitrogen, A11122) followed by a 45 min incubation in Alexa Fluor 488 donkey-α-rabbit IgG (Invitrogen, A21206). Immunofluorescence of mounted cover-slips was acquired on a Zeiss LSM 510 confocal microscope (Zeiss, Plan-Neofluar 40×/0.75).

References

1. Nagel, G. et al. Channelrhodopsin-2, a directly light-gated cation-selective membrane channel. *Proc Natl Acad Sci USA* **100**, 13940-13945 (2003).
2. Nagel, G. et al. Light activation of channelrhodopsin-2 in excitable cells of *Caenorhabditis elegans* triggers rapid behavioral responses. *Curr Biol* **15**, 2279-2284 (2005).
3. Boyden, E., Zhang, F., Bamberg, E., Nagel, G. & Deisseroth, K. Millisecond-timescale, genetically targeted optical control of neural activity. *Nat Neurosci* **8**, 1263-1268 (2005).
4. Zhang, F. et al. Multimodal fast optical interrogation of neural circuitry. *Nature* **446**, 633-639 (2007).
5. Bamann, C., Gueta, R., Kleinlogel, S., Nagel, G. & Bamberg, E. Structural guidance of the photocycle of channelrhodopsin-2 by an interhelical hydrogen bond. *Biochemistry* **49**, 267-278 (2010).
6. Berndt, A., Yizhar, O., Gunaydin, L., Hegemann, P. & Deisseroth, K. Bi-stable neural state switches. *Nat Neurosci* **12**, 229-234 (2009).
7. Lin, J., Lin, M., Steinbach, P. & Tsien, R. Characterization of engineered channelrhodopsin variants with improved properties and kinetics. *Biophys J* **96**, 1803-1814 (2009).
8. Lagali, P. et al. Light-activated channels targeted to ON bipolar cells restore visual function in retinal degeneration *Nat Neurosci* **11**, 667-675 (2008).
9. Bi, A. et al. Ectopic expression of a microbial-type rhodopsin restores visual responses in mice with photoreceptor degeneration. *Neuron* **50**, 23-33 (2006).
10. Frankenhäuser, B. & Hodgkin, A. The action of calcium on the electrical properties of squid axons. *J Physiol (Lond)* **137**, 218-244 (1957).
11. Hille, B. Ion channels of excitable membranes 3rd edn 649-662 (Sinauer Associates, Sunderland Massachusetts USA, 2001).
12. Gunaydin, L. et al. Ultrafast optogenetic control. *Nat Neurosci* **13**, 387-392 (2010).
13. Bamann, C., Kirsch, T., Nagel, G. & Bamberg, E. Spectral characteristics of the photocycle of channelrhodopsin-2 and its implication for channel function. *J Mol Biol* **375**, 686-694 (2008).
14. Feldbauer, K. et al. Channelrhodopsin-2 is a leaky proton pump. *Proc Natl Acad Sci USA* (2009).
15. Caldwell, J. et al. Increases in intracellular calcium triggered by channelrhodopsin-2 potentiate the response of metabotropic glutamate receptor mGluR7. *J Biol Chemistry* **283**, 2430024307 (2008).
16. Weber, W.-M. Ion currents in *Xenopus laevis* oocytes: state of the art. *Biochim Biophys Acta* **1421**, 213-233 (1999).
17. Thyagarajan, S. et al. Visual function in mice with photoreceptor degeneration and transgenic expression of channelrhodopsin 2 in ganglion cells. *J Neurosci* **30**, 8745-8758 (2010).
18. Hille, B., Woodhull, B. & Shapiro, B. Negative surface charge near sodium channels of nerve: divalent ions, monovalent ions, and pH. *Philos Trans R Soc Lond B Biol Sci* **270**, 301-318 (1975).

19.   Muller, R. & Finkelstein, A. The effect of surface charge on the voltage-dependent conductance induced in thin lipid membranes by monazomycin. *J General Physiol* **60**, 285-306 (1972).

20.   Faber, E. & Sah, P. Calcium-activateed potassium-channels: multiple contributions to neuronal function. *Neuroscientist* **9**, 181-194 (2003).

21.   Joh, N., Oberai, A., Yang, D., Whitelegge, J. & Bowie, J. Similar energetic contributions of packing in the core of membrane and water-soluble proteins. *J Am Chem Soc* **131**, 10846–10847 (2009).

22.   Subramaniam, S., Faruqi, A., Oesterhelt, D. & Henderson, R. Electron diffraction studies of light-induced conformational changes in the Leu-93→Ala bacteriorhodopsin mutant. *Proc Nat Acad Sci USA* **94** 1767-1772 (1997).

23.   Subramaniam, S., Greenhalgh, D., Rath, P., Rothschild, K. & Khorana, H. Replacement of leucine-93 by alanine or threonine slows down the decay of the N and O intermediates in the photocycle of bacteriorhodopsin: implications for proton uptake and 13-cis-retinal all-trans-retinal reisomerization. *Proc Natl Acad Sci USA* **88**, 6873-6877 (1991).

24.   Nack, M. et al. The DC gate in Channelrhodopsin-2: crucial hydrogen bonding interaction between C128 and D156. *Photochemical & Photobiological Sciences* **9**, 194-198 (2010).

25.   Cady, C., Evans, M.S. & Brewer, G.J. Age-related differences in NMDA responses in cultured rat hippocampal neurons. *Brain Research* **921**, 1-11 (2001).

26.   Busskamp, V. et al. Genetic reactivation of cone photoreceptors restores visual responses in retinitis pigmentosa. . *Science* **329**, 413-417 (2010).

27.   Humphrey, W., Dalke, A. and Schulten, K. VMD - Visual Molecular Dynamics. *J Molec Graphics* **14**, 33-38 (1996).

28.   Lorenz, C., Pusch, M. & Jentsch, T. Heteromultimeric ClC chloride channels with novel properties. *Proc Natl Acad Sci USA* **92**, 13362-13366 (1996).

29.   Allocca, M. et al. Novel adeno-associated virus serotypes efficiently transduce murine photoreceptors. *J Virology* **81**, 11372–11380 (2007).

30.   de Felipe, P. et al. E unum pluribus: multiple proteins from a self-processing polyprotein. *Trends Biotechnol* **24**, 68-75 (2006).
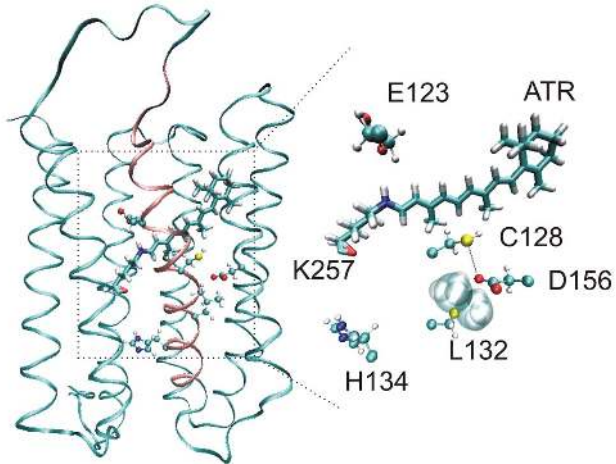
Supplementary Information

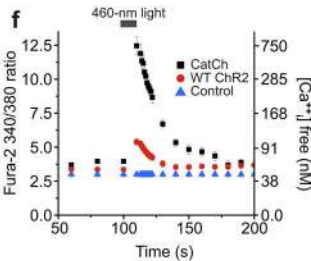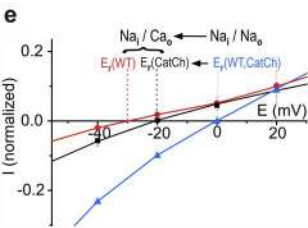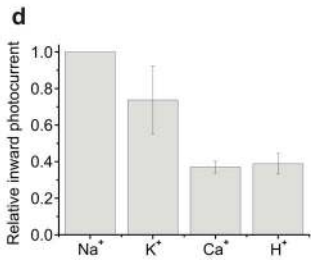**Supplementary Figure 1.** Spectroscopic characterization of CatCh.
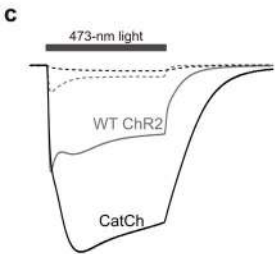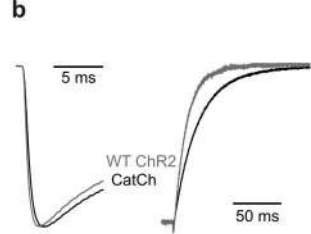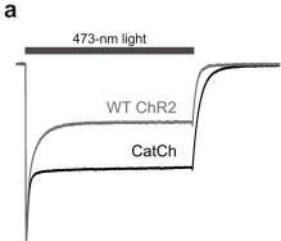
Supplementary Figure 2. Action spectrum of CatCh.

Supplementary Figure 3. Surface potential changes induced by Ca^{++}.

Supplementary Note. Estimation of the Ca^{++}-influx into a neuron through CatCh during illumination.

Supplementary Discussion. Possible effects of CatCh activity on synaptic plasticity.

E123 ATR
K257
C128
D156
L132
H134

a

473-nm light

WT ChR2

CatCh

b

5 ms

WT ChR2

CatCh

50 ms

c

473-nm light

WT ChR2

CatCh

d

Relative inward photocurrent

Na$^+$ K$^+$ Ca$^+$ H$^+$

e

I (normalized)

Na$_i$ / Ca$_o$ ← Na$_i$ / Na$_o$

E$_r$(WT)   E$_r$(CatCh)   E$_r$(WT,CatCh)

0.2

0.0

-0.2

-40   -20   0   20   E (mV)

f

460-nm light

Fura-2 340/380 ratio

[Ca^{2+}]$_{free}$ (nM)

CatCh

WT ChR2

Control

12.5

10.0

7.5

5.0

2.5

750

285

168

91

38

50   100   150   200   Time (s)

a

b

473-nm light

WT ChR2

CatCh

200 pA

200 ms

a

473-nm light

b

473-nm light

c

d

532-nm light

e

f

g

h

−63 mV

i

Ca²⁺

Mg²⁺

Prolonged depolarisation

Extra spikes

Table 1: Comparison of properties of CatCh with other excitatory optogenetic tools

		τ_{on} [ms]	τ_{off} [ms,s]	γ [fS]	I (pA) stat	I_{stat}/I_{max}	λ_{max} (nm)	J (ph s^{-1} cm^{-2}) [EC50 (mW/mm^2)]	max spike υ	p_{Ca}/p_{Na}	AD	Ref
CaTCh		0.6 ± 0.003	16 ± 3 ms	140 ± 5	643.8 ± 30.9	0.69 ± 0.20	474	$10^{16}-10^{17}$ 70x lower wt [0.7]	≥ 50 Hz	0.24	No	
WT ChR2		0.2 ± 0.002	10 ± 1 ms	$\sim150^{b}$	216.3 ± 39.0	0.37 ± 0.18	470	$5\times10^{17}-10^{19}$ [0.7]	≤ 20 Hz	0.15	Yes	[1,3,14]
ChR2 H134R		~0.6	19 ± 2 ms	$\sim150^{b}$	~ 1.5 x I_{wt}	0.53 ± 0.09	450	$5\times10^{17}-10^{19}$ [0.7]	~ 20 Hz	—	Yes	[2,7,14]
SFO's, slow mutants	C128T	9 ± 1.6	2 ± 0.5 s	—	~ 0.73 x I_{wt}	~ 0.5	480	$5\times10^{17}-10^{19}$ [0.03]	c	—	Yes	[5,6]
	C128A	5.7 ± 1.0	52 ± 2 s	—	~ 0.30 x I_{wt}	~ 0.7	480	$5\times10^{17}-10^{19}$ [0.01]	c	—	Yes	
	C128S	30 ± 7.5	106 ± 9 s	—	~ 0.25 x I_{wt}	~ 0.85	480	$5\times10^{17}-10^{19}$ [0.01]	c	—	Yes	
	D156A	3.3 ± 0.1	>150 s^{a}	—	$\sim I_{wt}$	~ 1	480	$5\times10^{17}-10^{19}$ [0.01]	d	—	Yes	
ChETA		—	4.8 ± 0.6 ms	—	~ 0.9 x I_{wt}	0.6 ± 0.04	500	$10^{18}-10^{19}$ less sensitive than wt	200 Hz	—	No	[12]
ChIEF		—	9.8 ± 0.7 ms	—	~ 3 x I_{wt}	~ 0.8	450	$10^{18}-10^{19}$ less sensitive than wt [0.92]	25 Hz	0.12	Yes	[7]

τ_{on}: values from single turnover measurements, γ: in 200 mM guanidine-HCl, RT, -60 mV **I:** HCN, -60 mV; $I_{wt} \equiv$ WT ChR2 current under respective experimental conditions, J: light intensity required to induce action potential; EC50: apparent half-saturating light intensities, **max spike υ:** maximal light-pulse induced reliable spike frequency, AD: artificial after depolarization, ^{a}data cannot be determined accurately and represents lower limit estimation, ^{b}extrapolated value, ^{c}subthreshold depolarization, ^{d}two-color on/off control with blue-yellow